THE JOURNAL OF BIOLOGICAL CHEMISTRY VOL. 289, NO. 33, pp. 23086–23096, August 15, 2014

Depletion of Cyclophilins B and C Leads to Dysregulation of Endoplasmic Reticulum Redox Homeostasis*

Received for publication, April 2, 2014, and in revised form, July 2, 2014 Published, JBC Papers in Press, July 2, 2014, DOI 10.1074/jbc.M114.570911

Pawel Stocki[1], **Daniel C. Chapman, Lori A. Beach, and David B. Williams**[2]

From the Department of Biochemistry, University of Toronto, Toronto M5S 1A8, Canada

Background: Cyclophilins catalyze *cis-trans* isomerization of peptidyl-prolyl bonds.
Results: Depletion of cyclophilins B and C results in endoplasmic reticulum (ER) hyperoxidation including more oxidized protein-disulfide isomerase enzymes and elevated oxidized:total glutathione ratio.
Conclusion: Cyclophilins B and C participate in ER redox homeostasis.
Significance: An unexpected level of ER redox regulation is revealed that likely contributes to cyclosporine A-induced oxidative stress.

Protein folding within the endoplasmic reticulum is assisted by molecular chaperones and folding catalysts that include members of the protein-disulfide isomerase and peptidyl-prolyl isomerase families. In this report, we examined the contributions of the cyclophilin subset of peptidyl-prolyl isomerases to protein folding and identified cyclophilin C as an endoplasmic reticulum (ER) cyclophilin in addition to cyclophilin B. Using albumin and transferrin as models of *cis*-proline-containing proteins in human hepatoma cells, we found that combined knockdown of cyclophilins B and C delayed transferrin secretion but surprisingly resulted in more efficient oxidative folding and secretion of albumin. Examination of the oxidation status of ER protein-disulfide isomerase family members revealed a shift to a more oxidized state. This was accompanied by a >5-fold elevation in the ratio of oxidized to total glutathione. This "hyperoxidation" phenotype could be duplicated by incubating cells with the cyclophilin inhibitor cyclosporine A, a treatment that triggered efficient ER depletion of cyclophilins B and C by inducing their secretion to the medium. To identify the pathway responsible for ER hyperoxidation, we individually depleted several enzymes that are known or suspected to deliver oxidizing equivalents to the ER: Ero1$\alpha\beta$, VKOR, PRDX4, or QSOX1. Remarkably, none of these enzymes contributed to the elevated oxidized to total glutathione ratio induced by cyclosporine A treatment. These findings establish cyclophilin C as an ER cyclophilin, demonstrate the novel involvement of cyclophilins B and C in ER redox homeostasis, and suggest the existence of an additional ER oxidative pathway that is modulated by ER cyclophilins.

Proteins entering the secretory pathway must fold and undergo a variety of modifications within the endoplasmic reticulum (ER)[3] to reach their native state. Such modifications include glycosylation, formation of disulfide bonds, and *cis-trans* isomerization of peptidyl-prolyl bonds. These processes are orchestrated by networks of ER-residing molecular chaperones and folding catalysts. The former function to prevent aggregation during folding as well as to coordinate the action of some of the folding catalysts. The latter include the protein-disulfide isomerases (PDIs), which catalyze the formation, isomerization, and reduction of disulfide bonds, as well as the peptidyl-prolyl isomerases (PPIs) that catalyze *cis-trans* interconversion of peptide bonds N-terminal to proline. Protein folding in the ER is subject to a stringent quality control system that retains misfolded proteins and targets them for proteasome-mediated degradation in the cytosol, a process termed ER-associated degradation (ERAD) (1). This complex process also involves the action of molecular chaperones to recognize misfolded substrates as well as the activities of certain PDI and PPI family members, apparently to assist in the unfolding of substrates prior to their retrotranslocation to the cytosol.

The PDIs constitute a large and diverse family of thiol oxidoreductases, with more than 20 members identified within the mammalian ER. PDIs contain at least one thioredoxin domain with catalytic activity determined by an active site C*XX*C motif. This motif must be in an oxidized, disulfide state to catalyze disulfide formation in substrates and in a reduced, dithiol state to catalyze disulfide reduction or isomerization (2). The large number of PDI family members appears to reflect distinct roles in the formation or reduction of disulfides during folding and ERAD, respectively, as well as differences in specificity for the diversity of folding proteins they encounter. For example, both PDI and ERp57 have well established roles in the oxidative folding of proteins (3–6), whereas ERdj5 functions primarily as a reductase in cooperation with the ER Hsp70 BiP to remove

* This work was supported in part by grants from the Canadian Cancer Society and the Canadian Institutes of Health Research.
[1] Supported by a fellowship from the Canadian Institutes of Health Research Training Program in Protein Folding and Interaction Dynamics.
[2] To whom correspondence should be addressed: Medical Sciences Bldg., University of Toronto, Toronto, Ontario M5S 1A8, Canada. Tel.: 416-978-2546; Fax: 416-978-8548; E-mail: david.williams@utoronto.ca.

[3] The abbreviations used are: ER, endoplasmic reticulum; Ero1, ER oxidoreductin; NEM, *N*-ethylmaleimide; PDI, protein-disulfide isomerase; PRDX4, peroxiredoxin IV; QSOX1, quiescin-sulfhydryl oxidase 1; UPR, unfolded protein response; VKOR, vitamin K epoxide reductase; Tm, tunicamycin; BFA, brefeldin A; PNGase F, peptide:*N*-glycosidase F; Endo H, endoglycosidase H; Tg, thapsigargin; TCEP, tris(2-carboxyethyl)phosphine; AMS, 4-acetamido-4′-maleimidylstilbene-2,2′-disulfonic acid; PPI, peptidyl-prolyl isomerase; ERAD, ER-associated degradation; FKBP, FK506-binding protein; Cyp, cyclophilin.

aberrant disulfides during protein folding (7) as well as from misfolded substrates during ERAD (8). Differences in specificity are best illustrated by ERp57, a PDI member that binds to the glycoprotein-selective chaperones calnexin and calreticulin, and as a consequence exhibits a strong preference for Asn-linked glycoprotein substrates (6, 9, 10).

For PDIs to catalyze formation of disulfide bonds in newly synthesized proteins, their active sites must be oxidized by one or more oxidant enzymes within the ER. In yeast, this process is carried out by the essential enzyme ER oxidoreductin 1 (Ero1), a flavoprotein that transfers oxidizing equivalents from molecular oxygen to reduced PDI with concomitant production of H_2O_2 (11, 12). However, mouse knockouts of the Ero1α and -β homologs are viable and exhibit only minor deficiencies in the oxidative folding of ER-traversing proteins (13). Consequently, potential complementary activities were examined as contributors to the PDI member oxidation process, including peroxiredoxin IV (PRDX4), quiescin-sulfhydryl oxidase 1 (QSOX1), and vitamin K epoxide reductase (VKOR) (14). PRDX4 uses H_2O_2 generated by Ero1 and other activities to form an interchain disulfide that can be donated to PDI family members (15). Consistent with a role in PDI member oxidation, depletion of PRDX4 exacerbated the phenotype of Ero1$\alpha\beta$ knock-out cells resulting in impaired growth, hypersensitivity to reducing agents, and impaired collagen secretion (13). Recently, VKOR has also been shown to contribute to protein disulfide formation in human hepatoma cells (16). VKOR catalyzes the reduction of vitamin K epoxide, resulting in the oxidation of a C*XX*C motif that may be transferred to certain PDI members (17–19). In contrast, the same study was unable to detect a similar role for QSOX1, an enzyme that uses molecular oxygen to oxidize an internal thioredoxin active site for transfer to a variety of substrates *in vitro*, accompanied by the production of H_2O_2 (20).

The other major family of protein folding catalysts in the ER is the PPIs that consist of parvulins, cyclophilins (Cyps), and FK506-binding proteins (FKBPs). The latter two groups are distinguished by their abilities to bind the immunosuppressive drugs cyclosporine A (CsA) or FK506, respectively. Immunosuppression is caused by the binding of drug-PPI complexes to cytosolic calcineurin, inhibiting its phosphatase activity and resulting in inactivation of the nuclear factor of activated T cells that is required for T cell activation (21, 22). *In vitro*, PPIs accelerate rate-limiting *cis-trans* proline interconversion during the folding of various protein substrates (23). In cells, these enzymes often facilitate the interconversion of a protein between alternative conformations that have distinct functions. For example, the cytosolic Pin1 PPI binds selectively to phosphorylated Ser/Thr-Pro motifs, catalyzing conformational changes that influence a wide array of cellular processes including cell growth, signal transduction, gene expression, immune responses, and neuronal function (24). Much less is known about PPI function within the ER where there are six luminal FKBPs (FKBP13, -19, -22, -23, -60, and -65) (25) and only one clearly established cyclophilin, CypB (26, 27). FKBP65 has been shown to associate with collagen and tropoelastin, interactions that *in vitro* can mildly enhance collage triple helix formation and initiate coacervation of tropoelastin (28, 29). However, most of the evidence for ER PPI function comes from studies on CypB. For example, the *Drosophila melanogaster* CypB homolog NinaA associates with rhodopsin in photoreceptor cells and is essential for rhodopsin export from the ER (30). CypB has also been shown to associate with the Na^+-dicarboxylate cotransporter in HEK293 cells and either CsA treatment or CypB knockdown dramatically reduced receptor expression (31). *In vitro*, CypB cooperates with PDI family member ERp72 to accelerate the assembly of disulfide-linked IgG C_H1-C_L heterodimers (32). In addition, CypB utilizes its PPIase activity in cooperation with BiP to accelerate the folding of the IgG C_H1 domain following its interaction with the light chain C_L domain (33). Recently, CypB has been shown to play a significant role in ERAD. CsA treatment or specific depletion of CypB delayed the degradation of *cis*-Pro-containing soluble but not membrane-bound misfolded proteins (34).

The *in vitro* experiments highlighting CypB cooperation with BiP and ERp72 are consistent with the finding of large complexes within the ER containing multiple chaperones and folding catalysts including BiP, Grp94, Grp170, co-chaperone ERdj3, and PDI members ERp72, P5, and PDI, and CypB (32, 35). In addition, CypB has been shown to use a conserved surface to interact with multiple partners including calnexin, calreticulin, Grp94, BiP, ERp72, PDI, and P5 (32, 36). Indeed, interactions between PDI and PPI family members extend beyond CypB to several ER FKBPs as well (32). Presumably, such interactions increase the efficiency of chaperone/foldase functions during folding and ERAD processes.

In this report we focus on the functions of ER cyclophilins and identify a second ER-residing cyclophilin, CypC. Combined siRNA-mediated depletion of CypB and CypC unexpectedly accelerated oxidative folding and secretion of albumin. This prompted an examination of PDI family members and we discovered that all enzymes tested had shifted to a more oxidized state, and indeed, the ER was hyperoxidized as exemplified by a dramatic increase in oxidized to total glutathione ratio. This phenomenon could be duplicated by treating cells with the cyclophilin inhibitor CsA. Neither Ero1, PRDX4, VKOR, nor QSOX1 were responsible for the hyperoxidation, suggesting the existence of an additional oxidative pathway that is modulated by ER cyclophilins.

EXPERIMENTAL PROCEDURES

Cell Lines—The human hepatoma cell line HepG2 was cultured in high glucose DMEM (Invitrogen) supplemented with 100 IU/ml of penicillin, 100 μg/ml of streptomycin, 2 mM L-glutamine, and 10% fetal bovine serum. The cells were incubated at 37 °C in a humidified 5% CO_2 atmosphere.

Antibodies and Other Materials—The following commercial antibodies were used in this study: anti-CypC (Proteintech, Chicago, IL) that was found to detect cyclophilins A, B, and C and was thus designated anti-PPIs, anti-CypB (Abcam, Cambridge, MA), anti-CypA (Abcam), anti-albumin (Sigma), anti-transferrin (Sigma), anti-GAPDH (Millipore Inc., Billerica, MA), anti-PrP (Cedarlane, Burlington, ON, Canada; mAb 3F4), anti-ERp72 (AssayDesigns, Farmingdale, NY), anti-P5 (Thermo Scientific, Rockford, IL), anti-Ero1α (Abcam), and anti-PRDX4 (Abcam). Anti-MHC class I free heavy chain and

anti-HA monoclonal antibodies were purified from hybridomas HC10 (37) and 12CA5, respectively. Rabbit antiserum directed against mouse ERp57 has been described previously (38). Rabbit anti-Ero1β (39) and anti-VKOR (40) were gifts of Dr. David Ron (University of Cambridge, Cambridge, UK) and Dr. Kathleen Berkner (Cleveland Clinic, Cleveland, Ohio), respectively. Rabbit anti-human QSOX1a (41) was a gift from Dr. Neil Bulleid (University of Glasgow, Glasgow, UK). Other materials include CsA, FK506, and rapamycin from LC Laboratories and thapsigargin (Tg), tunicamycin (Tm) and brefeldin A (BFA) from Sigma. Peptide:*N*-glycosidase F (PNGase F) and endoglycosidase H (Endo H) (New England Biolabs, Whitby, ON, Canada) were used according to the manufacturer's instructions.

RNA Interference—Knockdowns were performed as previously described (5, 16). In brief, knockdowns used a total of 40 nM of specific (or mixed at the indicated ratios for double knockdowns) Stealth Select^{TM} siRNAs (Invitrogen) combined with 6 μl of Oligofectamine^{TM} (Invitrogen). For knockdowns of CypB, CypC, CypB + CypC (siRNAs mixed at a 1:3 ratio), PRDX4, and VKOR, HepG2 cells were transfected on day 1 and again on day 4 followed by analysis on day 7. For knockdown of QSOX1 (both a and b forms), the cells were transfected on day 1 and analyzed on day 4. Double knockdown of Ero1α and Ero1β was done by treating the cells with a 1:1 mixture of specific siRNAs on day 1, then only Ero1α on day 4, and only Ero1β on day 5 for analysis on day 7. Control transfections were performed with non-targeting negative control Stealth Select siRNA (Invitrogen).

Pulse-Chase Radiolabeling and Immunoisolation—HepG2 cells were grown on 60-mm plates overnight to 70–80% confluence, starved for 30 min in Met-free RPMI 1640, then radiolabeled for 10 min at 37 °C with 0.1 mCi/ml of [^{35}S]Met (PerkinElmer Life Sciences, >1,000 Ci/mmol) in starvation medium. Chases were initiated by the addition of pre-warmed RPMI 1640 supplemented with 10% fetal bovine serum and an additional 1 mM Met. The chases were stopped by placing the plates on ice and incubating with 2 ml of ice-cold PBS containing 20 mM *N*-ethylmaleimide (NEM) (Sigma) for 3 min. The cells were then lysed for 30 min in RIPA buffer (50 mM Tris, pH 7.4, 150 mM NaCl, 1 mM EDTA, 1% Nonidet P-40, 0.25% sodium deoxycholate, 0.1% SDS, and protease inhibitors) containing 20 mM NEM and 10 mM iodoacetamide (IAA) (Sigma-Aldrich) and centrifuged at 10,000 × *g* for 10 min. The media samples and lysate supernatants were subjected to immunoisolation with 30 μg of anti-albumin or anti-transferrin antibodies for 2 h followed by a 1-h incubation with 30 μl of protein A-agarose beads (GE Healthcare). The beads were then washed three times with 50 mM Tris, pH 7.4, 150 mM NaCl, 1 mM EDTA, 0.1% Nonidet P-40, 0.025% deoxycholate, 0.01% SDS, and eluted in SDS-PAGE sample buffer either lacking or containing 40 mM DTT. Proteins were separated using 10% SDS-PAGE gels, which were dried, exposed on photostimulable phosphor plates, and analyzed on a Typhoon Trio+ phosphorimager (GE Healthcare). Quantification was performed using Quantity One software (Bio-Rad).

Digitonin Membrane Permeabilization—HepG2 cells (1×10^7) were incubated for 30 min with gentle rocking at room temperature in 7 ml of PBS containing digitonin (Sigma) at concentrations of 0, 0.003, 0.006, or 0.009%. The cells were then centrifuged, and the pellets were lysed in RIPA buffer followed by immunoblot analysis to detect various cyclophilins.

Detection of Unfolded Protein Response-Xbp1 Splicing Assay—The assay was performed as previously described (5). In brief, total RNA was isolated from HepG2 cells using the RNeasy kit (Qiagen, Toronto, ON, Canada) and subjected to one-step reverse transcription PCR (Qiagen) using human Xbp1 amplification primers: 5′-GGAGTTAAGACAGCGCTTGG-3′ and 5′-GAGATGTTCTGGAGGGGTGA-3′. As a positive control, 3 mM DTT was added to the medium of HepG2 cells for 2 h. Alternatively, where indicated, 3 μM Tg or 5 μg/ml of Tm was incubated with the cells overnight. Dimethyl sulfoxide was used as vehicle control.

Evaluation of PDI Family Member Redox State—Cells were rinsed with PBS and then incubated with 20 mM NEM in ice-cold PBS for 10 min to alkylate free protein thiols, followed by lysis in RIPA buffer. The lysates were adjusted to 1% SDS, and 10 mM tris(2-carboxyethyl)phosphine (TCEP) (Sigma) was added to reduce protein disulfides before the lysates were boiled for 3 min. 4-Acetamido-4′-maleimidylstilbene-2,2′-disulfonic acid (AMS, 25 mM; Sigma) was then added for 1 h at room temperature to alkylate the newly exposed thiol groups. As positive or negative controls, cells were pre-incubated with 5 mM diamide or 5 mM DTT for 5 min at 37 °C, respectively, and then processed as above. Samples were analyzed using 7.5% non-reducing SDS-PAGE gels and subsequently immunoblotted to detect various PDI family members.

Glutathione Levels—Oxidized glutathione (GSSG) and total glutathione (GSSG + GSH) levels were measured as described before (16). In brief, the cells were washed in PBS, scraped off the plates, and resuspended in 50 μl of 5% 5-sulfosalicyclic acid. Following centrifugation, the supernatant fraction was recovered and diluted with 330 μl of 0.1 M sodium phosphate buffer, pH 7.4, containing 1 mM EDTA (PE buffer). To assay total glutathione, 50 μl of sample was added directly to the wells of a flat bottom 96-well plate. To measure GSSG, 6 μl of 2-vinylpyridine (Sigma) was added to 130 μl of each sample, incubated for 1 h at room temperature, and then a 50-μl aliquot was used for the analysis in the 96-well plate. To each well, 100 μl of reaction mixture was added (2.8 ml of 1 mM Ellman's reagent (5,5′-dithiobis(2-nitrobenzoic acid)), 3.75 ml of 1 mM NADPH, 20 units of glutathione reductase, and 5.85 ml of PE buffer; all reagents from Sigma). Absorbance at 405 nm was recorded continuously for 5 min. Initial reaction rates were compared with those obtained with a standard curve spanning 0–500 pmol of GSSG.

Statistical Analysis—Statistical significance was assessed with the two-tailed, paired Student's *t* test for at least three independently performed experiments, and p value <0.05 was considered significant.

RESULTS

Cyclophilin C Resides within the Early Secretory Pathway—Prior to examining the involvement of ER cyclophilins in protein folding, we addressed the question of whether cyclophilins other than CypB may be functioning within this organelle.

Analysis of the cyclophilin family using the SignalP 4.0 online prediction tool (42) revealed that, in addition to CypB, CypC contains a potential N-terminal signal sequence that could direct it into the ER. Indeed, early work suggested a potential ER localization for CypC (43) and had confirmed its enzymatic activity and inhibition by CsA (44), but most subsequent studies assumed a cytosolic location and it is annotated as such in UniProt (accession P30412). We used a commercially available anti-CypC antibody to aid in its localization but found that the antibody is not specific. As shown in Fig. 1*A* (mock), when used for immunoblotting lysates of human hepatoma HepG2 cells, it detected multiple protein bands with the fastest migrating species identified as cytosolic CypA (verified in a parallel blot using anti-CypA antiserum, data not shown). Knockdowns of either CypB or CypC using specific siRNAs revealed that the species migrating closest to CypA was CypB, whereas two other major bands, which sometimes resolved as doublets, could be attributed to CypC (Fig. 1*A*). Given that the anti-CypC antibody cross-reacted with CypB and CypA, we subsequently refer to this antibody as "anti-PPIs." The lower CypC doublet migrated near the predicted size for CypC of 20 kDa, however, the upper band suggested post-translational modification, possibly *N*-glycosylation. CypC possesses two potential *N*-glycosylation sites, and indeed, digestion of cell lysates with PNGase F to remove attached *N*-glycans collapsed the upper band into the low molecular weight CypC species (Fig. 1*B*, *right panel*). Digestion of the cellular prion glycoprotein (PrP) served as a positive control for PNGase F activity, whereas unglycosylated CypB was used as a negative control (Fig. 1*B*).

The presence of glycosylated and unglycosylated forms of CypC might be a consequence of their localizations to different cellular compartments, *i.e.* glycosylated CypC would be expected to localize to or traverse the ER, whereas unglycosylated CypC may reside in the cytosol. It is also possible that both species may have translocated into the ER, but glycosylation is simply inefficient. To distinguish between these possibilities, the plasma membrane of HepG2 cells was permeabilized with low concentrations of digitonin to release cytosolic proteins, whereas luminal proteins of the secretory pathway are retained. The cells were then lysed and immunoblotted for CypC as well as cytosolic CypA and ER-localized CypB. As expected, CypA was gradually lost as a function of increasing digitonin concentration but no loss of CypB was observed (Fig. 1*C*). Both species of CypC, glycosylated and unglycosylated, were retained even at the highest digitonin concentration, consistent with their localization within the secretory pathway (Fig. 1*C*). The enzyme Endo H selectively removes immature *N*-linked glycans from glycoproteins that reside within the ER or that have not traversed beyond the *medial* Golgi apparatus. Glycosylated CypC was fully sensitive to Endo H digestion consistent with its localization to the early secretory pathway, most likely the ER (Fig. 1*D*). In contrast, MHC class I molecules that progress beyond the *medial* Golgi to the cell surface and thus possess immature glycans as well as mature, Golgi-processed forms, were partially resistant to Endo H digestion (Fig. 1*D*).

Neither CypB nor CypC contain a "KDEL-like" ER localization signal and previous reports have variously attributed a localization signal on CypB to its C-terminal 10 residues (45) or

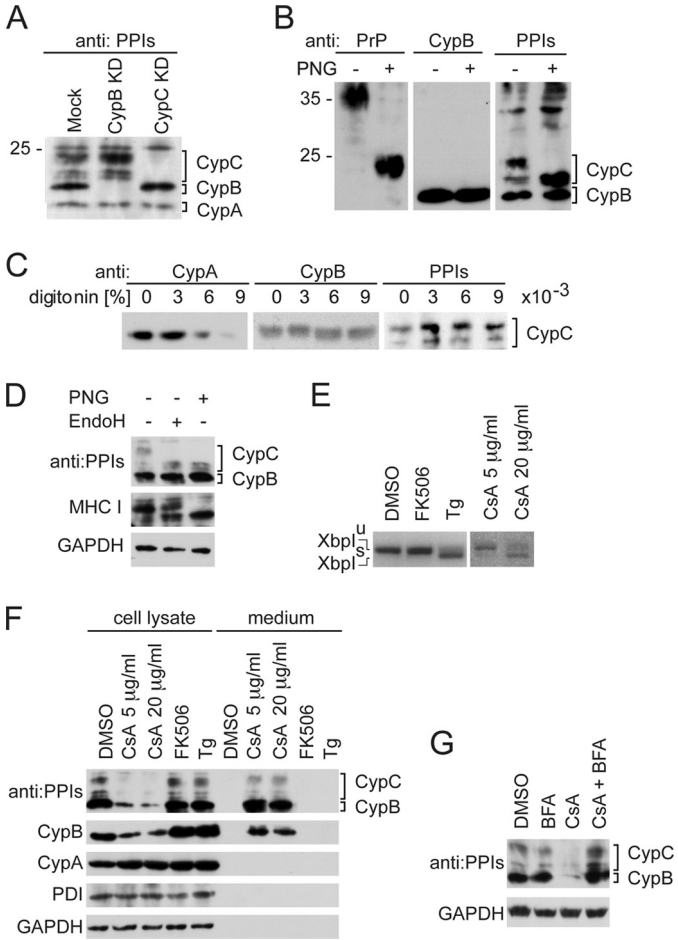

FIGURE 1. **CypB and CypC expression profile and localization in HepG2 cells.** *A*, immunoblotting was used to detect CypB and CypC in HepG2 cells. The specificity of the anti-PPIs antibodies for CypB and CypC was established by comparison of the band profiles of either CypB or CypC specific knockdowns (*KD*) *versus* a mock control. *B,* the *N*-glycosylation status of CypC was tested by PNGase F (*PNG*) digestion of cell lysates. Prion protein (*PrP*) and CypB were used as glycosylated and unglycosylated protein controls, respectively. *C,* to test if unglycosylated CypC is cytosolically localized, cells were treated for 30 min with the indicated concentrations of digitonin to selectively permeabilize the cell membrane and release cytosolic proteins. The cells were then lysed and analyzed by immunoblotting. CypA and CypB were used as cytosolic and ER-residing protein controls, respectively. *D,* glycosylated CypC possesses an endoglycosidase H-sensitive glycan. Cell lysates were digested with Endo H and PNGase F and analyzed by immunoblotting. MHC class I was used as a control glycoprotein that traverses the entire secretory pathway and GAPDH served as a loading control. *E*, UPR activation was tested in cells treated with CsA (5 or 20 μg/ml), FK506 (20 μg/ml), or thapsigargin (*Tg*; 3 μM) using an Xbp1 splicing assay. mRNA from the treated cells was isolated and tested for the splicing status of Xbp1 mRNA, unspliced (*Xbp1*^{u}) or spliced Xbp1 (*Xbp1*^{s}) indicate negative or positive UPR activation, respectively. *F*, the efficiency of CypB and CypC retention within the ER was assessed under different conditions. Cells were treated with CsA (5 or 20 μg/ml), FK506 (20 μg/ml), or Tg (3 μM) overnight. Cell lysate and media samples were tested by immunoblot for the relative levels of CypB and CypC as well as the ER luminal protein PDI. *G*, BFA blocks CsA-induced secretion of CypB and CypC. HepG2 cells were treated with 5 μg/ml of CsA and/or 0.5 μg/ml of BFA overnight and the cell lysates were tested for CypB and CypC retention. Dimethyl sulfoxide (*DMSO*) was used as a vehicle control.

to a Trp residue within the CsA binding site (46). Consistent with the latter finding, it has been reported that CsA treatment induces CypB secretion from the ER to the media in HeLa and BHK cells (27). We took advantage of this observation as an alternative means to localize CypC to the secretory pathway. As shown in Fig. 1*F*, treatment of HepG2 cells with 5 or 20 μg/ml of

CsA induced the secretion not only of CypB but also the glycosylated and unglycosylated forms of CypC. No secretion was observed for ER-resident PDI or cytosolic proteins CypA and GAPDH (Fig. 1*F*). This experiment confirmed that both glycosylated and unglycosylated forms of CypC reside within the secretory pathway. Secretion of CypB and CypC was not an indirect effect of CsA inducing the unfolded protein response (UPR) because 5 μg/ml of CsA resulted in robust secretion, but no induction of the UPR as measured by the splicing of the Xbp1 transcription factor (Fig. 1*E*). Furthermore, when the UPR was induced by Tg treatment, it failed to stimulate the secretion of CypB or CypC (Fig. 1, *E* and *F*). Likewise, inactivation of the cytosolic calcineurin-mediated signal transduction pathway by CsA did not play a important role in triggering the secretion of CypB and CypC because treatment with FK506, which inactivates the same pathway, did not induce secretion (Fig. 1*F*). It should be noted that non-induced minor leakage of CypC, but not CypB, to the media was occasionally observed (data not shown). Finally, we tested if the CsA-induced secretion of CypB and CypC was sensitive to BFA, a drug that blocks protein export from the ER. Secretion of CypB and both the glycosylated and unglycosylated forms of CypC were blocked upon BFA treatment, consistent with an ER localization for both proteins and confirming that the induced secretion mechanism utilizes the constitutive secretory pathway (Fig. 1*G*).

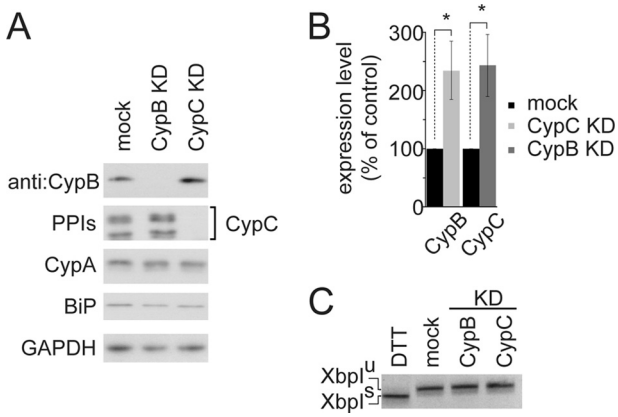

FIGURE 2. **Single knockdown of either CypB or CypC results in compensatory up-regulation of the remaining ER-residing cyclophilin in HepG2 cells.** *A*, CypB or CypC knockdown (*KD*) was performed using specific siRNA and compared with the mock knockdown performed with negative control siRNA. Knockdown efficiency was assessed by immunoblotting. CypA served as a knockdown specificity control, the ER Hsp70 BiP was used as a marker of UPR induction and GAPDH was a loading control. *B,* band intensities from the CypB and CypC immunoblots were quantified by densitometry, normalized to GAPDH levels, and expressed as a percentage change in expression as a function of the indicated knockdown condition ($n = 3$, $\pm$S.D.). *, indicates significant difference from control ($p < 0.05$). *C,* UPR activation was tested on day 6 in HepG2 cells depleted for either CypB or CypC using the Xbp1 splicing assay. HepG2 cells treated with 3 mM DTT for 2 h were used as a positive control for UPR induction.

Combined CypB and CypC Depletion Differentially Affects the Oxidative Folding and Secretion of Albumin and Transferrin—To investigate the role of CypB and CypC in protein folding within the ER, we used an siRNA approach to specifically knock down expression of the proteins alone or in combination in HepG2 cells. We observed that knockdown of either CypB or CypC resulted in significantly increased expression of the remaining ER-residing cyclophilin, whereas expression of cytosolic CypA was unaffected (Fig. 2, *A* and *B*). Importantly, the knockdown conditions did not cause UPR activation, which increases the expression of a variety of ER chaperones and folding catalysts, including CypB (47). This was evidenced by a lack of increase in BiP expression (Fig. 2*A*) or in Xbp1 splicing (Fig. 2*C*). These findings suggest that there are compensatory mechanisms to maintain cyclophilin activity within the ER.

Because there is no direct method to track *cis-trans* isomerization of prolines within the ER we used an indirect approach to evaluate the contributions of CypB and CypC to protein folding. Albumin and transferrin were chosen as model *cis*-Pro-containing proteins that undergo oxidative folding catalyzed mainly by PDI, ERp57, and ERp72 (5). Using pulse-chase radiolabeling, the efficiency of protein folding can be monitored by quantifying progressive increases in electrophoretic mobility that accompany disulfide formation, as well as subsequent secretion to the media. However, when this was performed in the context of single knockdowns of either CypB or CypC, there were no measurable changes in oxidative folding or secretion of either albumin or transferrin (data not shown). We speculated that single knockdowns of CypB or CypC did not produce any visible phenotype due to potential compensatory activities of CypB for CypC and vice versa. Accordingly, we performed a combined knockdown of both cyclophilins (Fig. 3*A*) and confirmed that there was no activation of the UPR under these conditions by monitoring both BiP expression (Fig. 3*A*) and Xbp1 splicing (Fig. 3*B*). The effects of combined CypB and -C depletion on the oxidative folding and secretion of albumin are shown in Fig. 3*C*. Note that the initial steps in albumin oxidation are very fast and it is not possible to capture the fully reduced form of albumin even in pulses as short as 3 min (5). Consequently, only partially oxidized (PO) intermediates and fully oxidized (O) species are visible. To visualize the reduced (*R*) form of albumin, DTT was added to certain samples prior to analysis. Surprisingly, depletion of CypB and CypC modestly increased the rate of albumin oxidative folding and also increased its rate of secretion to the media (Fig. 3*C*, quantified in *D* and *E*). In contrast, no effect of combined CypB and CypC depletion could be detected on the oxidative folding of transferrin, although we noted a slowing of its secretion (Fig. 3, *F* and *G*).

Combined CypB and CypC Depletion Results in ER Hyperoxidation—The increased rate of albumin folding and secretion upon cyclophilin depletion was unexpected because the few published studies using the cyclophilin inhibitor CsA or CypB depletion tended to impair production of functional proteins (30, 31, 48). Given that oxidative folding of albumin depends on PDI family members such as PDI and ERp72 (5), and that several family members associate with PPIs (32, 35), we speculated that ER cyclophilin depletion might somehow influence the activity of PDI members.

Accordingly, we assessed the oxidation state of several PDI family members under control conditions and following single or double knockdown of CypB and CypC (Fig. 4*A*). This was accomplished by first flooding cells with membrane-permeable NEM to alkylate free protein thiols then, following lysis, protein disulfides were reduced and alkylated with AMS. Due to the size of AMS, PDI members whose active sites were in the oxidized

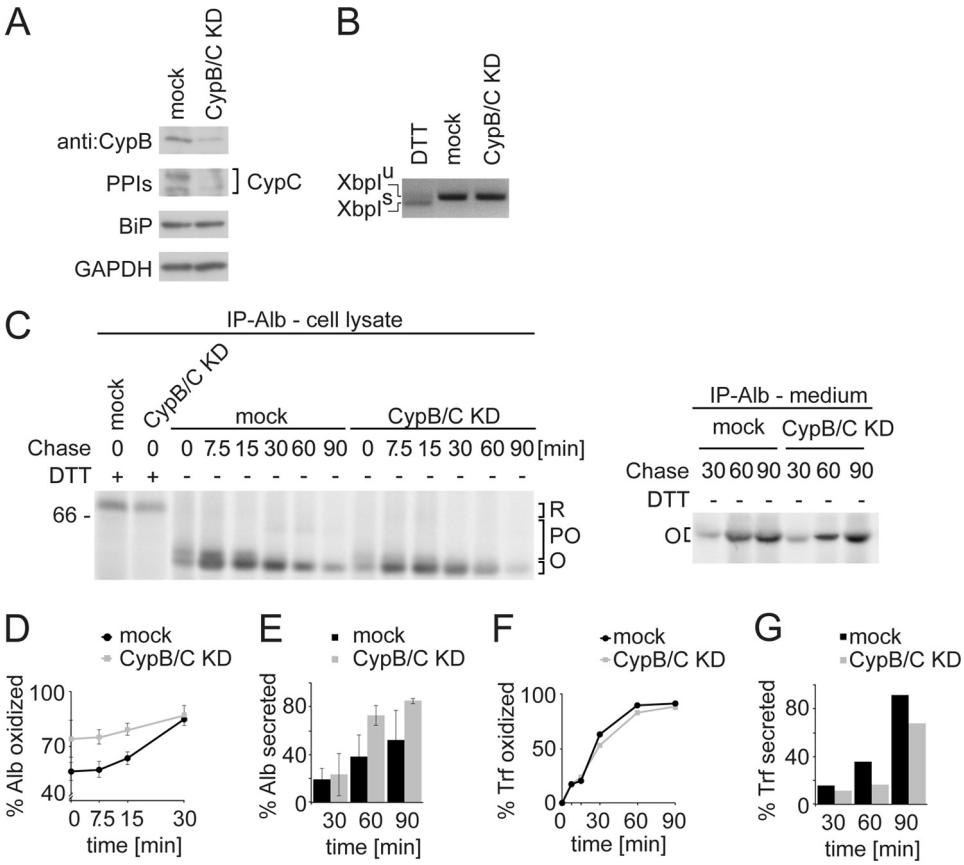

FIGURE 3. **Combined knockdown of CypB and CypC improves oxidative folding and secretion of albumin in HepG2 cells.** *A*, combined CypB and CypC knockdown (*CypB/C*) was performed using specific siRNAs and compared with the mock knockdown (*KD*) performed using negative control siRNA. The efficiency of the knockdown was assessed by immunoblotting. GAPDH was used as a loading control and BiP served as an indicator of UPR activation. *B*, UPR activation was additionally tested on day 6 in double knockdown cells using the Xbp1 splicing assay. HepG2 cells treated with 3 mM DTT for 2 h were used as a positive control. *C*, kinetics of albumin disulfide formation and secretion. Cells depleted of both CypB and CypC were radiolabeled with [^{35}S]Met for 10 min and then chased with unlabeled Met for the indicated times. NEM (20 mM) was added to alkylate free thiols and then albumin was immunoisolated from cell lysates and media. The samples were analyzed by SDS-PAGE gel under reducing (+*DTT*) or non-reducing (−*DTT*) conditions. The mobilities of reduced (*R*), partially oxidized (*PO*), and oxidized (*O*) forms of albumin are indicated. *D*, kinetics of albumin oxidation presented as the amount of fully oxidized protein in cells and media as a percentage of total radiolabeled albumin at each chase time ($n = 3$, ±S.D.). *E*, secretion kinetics of albumin presented as a percentage of total albumin signal at each chase time ($n = 3$, ±S.D.). *F*, the kinetics of transferrin oxidation were determined as described for albumin above and are presented as the amount of fully oxidized protein as a percentage of all forms of transferrin at each chase time ($n = 3$, ±S.D.). *G*, secretion kinetics of transferrin presented as a percentage of total transferrin signal at each chase time ($n = 3$, ±S.D.). Data are representative of two independent experiments.

disulfide state migrate more slowly on SDS-PAGE compared with when their active sites were reduced. As controls, cells were treated with either DTT or diamide, to reduce or oxidize PDIs, respectively. PDI members ERp72, ERp57, and P5 were used for this analysis because they exhibit significant mobility shifts following alkylation by AMS in contrast to PDI that shifts only minimally (49). Under control conditions, the active sites of ERp72, ERp57, and P5 were predominantly in the reduced state in HepG2 cells (Fig. 4*B*) as previously noted in other cell lines (50). Remarkably, although single knockdown of either CypB or CypC had no effect on the PDI member oxidation state, the double knockdown resulted in a shift of all tested PDIs to a more oxidized state. This phenomenon could be recapitulated by CsA treatment as shown for P5 (Fig. 4*C*), and ERp72 and ERp57 (Fig. 4*E*). This was unrelated to CsA induction of the UPR because it occurred at 5 μg/ml of CsA, which was too low to activate UPR responses (Fig. 4, *C* and *D*), and did not occur when the UPR was induced by Tm treatment (Fig. 4*C*). Likewise, neither FK506 nor rapamycin (Rapa) influenced the oxidation state of P5 (Fig. 4*C*).

The oxidation state of PDIs is influenced by the ER redox state, which can be measured by assessing the ratio of GSSG, which arises mainly from the ER (51, 52), to total glutathione (GS). We assessed the GSSG:GS ratio in cells depleted of both CypB and CypC and found it to be elevated 5-fold when compared with the non-depleted control (Fig. 4*F*). CsA treatment also increased the GSSG:GS ratio but, importantly, combined CsA treatment and double knockdown did not elevate the ratio more than double knockdown alone (Fig. 4*F*). Thus it can be assumed that a substantial portion of the CsA-mediated ER oxidation is due to its effects on CypB and CypC. We also tested whether combined depletion of CypB and CypC resulted in the generation of H_2O_2, which might be expected if ER oxidases such as Ero1 and QSOX1 were hyperactive (11, 12, 20). However, no increase in H_2O_2 production was observed as assessed using the Amplex Red fluorescent peroxide assay of the cell culture medium (data not shown).

Contribution of Candidate Oxidative Enzymes to CsA-mediated ER Hyperoxidation—We evaluated whether any of the known ER enzymes that deliver oxidizing equivalents to PDIs,

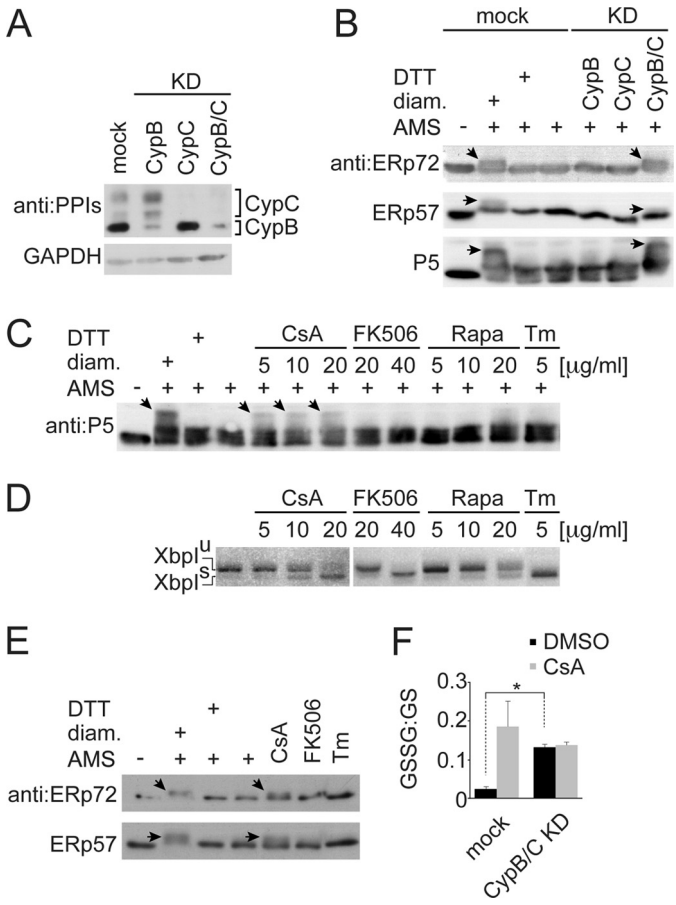

FIGURE 4. **CsA treatment or double knockdown of CypB and CypC results in increased oxidation of PDIs and an elevated GSSG:GS ratio in HepG2 cells.** *A,* single and double knockdown (*KD*) efficiencies of CypB and CypC were assessed by immunoblotting with GAPDH serving as a loading control. *B,* oxidation state of PDIs under single or double depletion of CypB and CypC. Before lysis, cells were incubated for 10 min with 20 mM NEM in ice-cold PBS to alkylate free protein thiols. Cells were then lysed and treated with TCEP to reduce disulfide bonds followed by treatment with the bulkier alkylating agent AMS to modify newly exposed thiol groups. The lysates were analyzed by SDS-PAGE and immunoblotted for ERp72, ERp57, and P5. The upward mobility shifts indicated by *arrows* represent an increase in the proportion of PDI members with oxidized active sites. As controls, before the NEM incubation, cells were treated for 5 min with either 5 mM DTT or 5 mM diamide (*diam.*) to reduce or oxidize PDIs, respectively. *C,* assessment of P5 oxidation state upon treatment with different PPI inhibitors. HepG2 cells were treated overnight with CsA, FK506, rapamycin (*Rapa*) or the UPR inducer Tm at the indicated concentrations. *D*, UPR activation was assessed by Xbp1 splicing assay under the same conditions as in *panel C*. *E,* assessment of the oxidation state of ERp72 and ERp57 upon overnight treatment with CsA (5 μg/ml), FK506 (20 μg/ml), or Tm (5 μg/ml). *F,* evaluation of the oxidation state of cellular glutathione. Cells depleted of CypB and CypC as well as mock knockdown cells were either left untreated or treated overnight with CsA (5 μg/ml). The cells were then lysed and the ratio of GSSG to total GS (*GSSG* + *GSH*) was determined ($n = 3$, $\pm$S.D.). *, indicates significant difference between mock and CypB/C combined knockdown ($p < 0.05$)

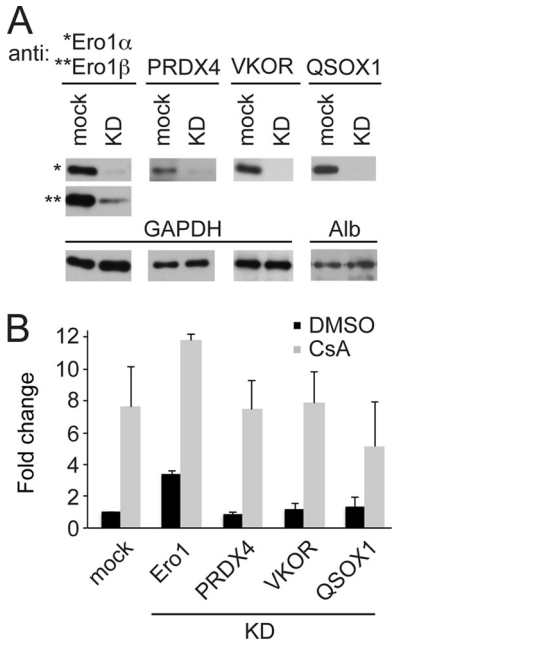

FIGURE 5. **Known ER oxidative enzymes do not contribute to the hyperoxidation arising from CsA treatment.** *A*, knockdown (*KD*) efficiency of ER oxidative enzymes. Knockdowns in HepG2 cells included double knockdown of Ero1α and Ero1β or single knockdown of PRDX4, secreted QSOX1, or VKOR. The efficiency of the knockdowns was assessed by immunoblotting with GAPDH or secreted albumin (in the case of QSOX1) serving as loading control. *B*, the indicated enzymes were depleted and then cells were incubated overnight in the absence or presence of CsA (5 μg/ml). The ratio of GSSG to total GS (*GSSG* + *GSH*) in cell lysates was assessed ($n = 3$, $\pm$S.D.).

and either directly or indirectly to glutathione, were playing a role in the observed cyclophilin-dependent hyperoxidation of the ER. Given the technical challenges of depleting candidate oxidant enzymes in combination with CypB and CypC knockdown, we used CsA to induce ER hyperoxidation. Although CsA has been shown to induce the production of reactive oxygen species by an uncertain mechanism (53–56), we showed above that CsA depletes CypB and CypC within the ER (Fig. 1). Furthermore, CsA treatment combined with CypB and CypC knockdown did not result in greater ER hyperoxidation than cyclophilin depletion alone (Fig. 4). Thus, a substantial portion of the CsA-mediated ER hyperoxidation is due to its effects on CypB and CypC.

Knockdown of each oxidant enzyme was performed and high efficiency depletion was observed for: Ero1 (both α and β isoforms), PRDX4, VKOR, and QSOX1 (Fig. 5*A*). Note that QSOX1 has been shown recently to be present predominantly in cell secretions in addition to modest levels within the secretory pathway (57) and thus the immunoblot represents secreted QSOX1 concentrated from culture media using concanavalin A-agarose beads. Knockdown cells were further treated in the absence or presence of CsA to assess whether any of these enzymes contribute to CsA-mediated ER hyperoxidation. Under control conditions lacking CsA, depletion of Ero1$\alpha\beta$ was accompanied by an increase in GSSG:GS ratio (Fig. 5*B*). This seemingly paradoxical finding has been noted previously, and presumably reflects the compensatory action of other oxidant systems upon loss of the predominant ER oxidase (16, 50). Following CsA treatment, it was surprising to observe that depletion of any of the four oxidant enzymes, Ero1$\alpha\beta$, PRDX4, VKOR, or QSOX1, had little impact on the ensuing hyperoxidation as reflected in the elevated GSSG:GS ratios (Fig. 5*B*). A modest reduction in the magnitude of the CsA response was observed in the case of QSOX1 depletion but this did not reach statistical significance. This suggests that one or more additional oxidative pathways exist that contribute to ER hyperoxidation under conditions of cyclophilin B and C depletion.

DISCUSSION

During the course of this study, we uncovered an additional ER-localized member of the cyclophilin family, CypC, that consists of two species: an Endo H-sensitive glycosylated form and an unglycosylated form. CypC has two potential *N*-glycosylation sites at residues 142 and 190. The latter residue is the likely glycosylation site because it is unique to CypC and is surface localized (PDB code 2ESL). In contrast, Asn-142 is shared with unglycosylated CypB and is buried within the protein. In HepG2 cells, unglycosylated CypC accounts for ~20–30% of the total protein. This could be due to inefficient glycosylation or it could be a consequence of inefficient translocation into the ER, thereby conferring a cytosolic localization for unglycosylated CypC. However, the latter possibility was excluded after we observed that the unglycosylated species was retained intracellularly upon plasma membrane permeabilization. Furthermore, both the glycosylated and unglycosylated species were secreted to the medium upon CsA treatment, and this secretion could be blocked by BFA. Additional efforts to localize CypC by immunofluorescence microscopy were hampered by the lack of a suitable antibody. We also transiently overexpressed N terminally epitope-tagged versions of CypB and CypC, but this produced localization artifacts because their secretion from the ER was no longer CsA inducible (data not shown).

The basis for CypB or CypC localization within the ER remains unclear. Neither protein possesses a canonical ER localization sequence, but CypB retention in the ER has been suggested to be conferred by a novel C-terminal motif (VEKPFAIAKE) (45). Alternatively, because CsA treatment induces CypB (27) and, as shown here, CypC secretion, it has been suggested that ER localization of CypB is regulated through its CsA binding site (46). However, mutations within either region did not substantially alter its ER distribution. The localization of CypB might be conferred in part through contact with other ER resident proteins because chemical cross-linking studies have identified CypB as a component of an extensive network of ER chaperones and folding catalysts that include BiP, Grp94, Grp170, co-chaperone ERdj3, and PDI members ERp72, P5, and PDI (35). Furthermore, using an ER membrane yeast two-hybrid assay and affinity purification methods a CypB interactome was identified that includes PDI, P5, ERp72, BiP, Grp94, calnexin, and calreticulin (32). CypB was found to interact with the tip of the arm domains of calnexin and calreticulin via a positively charged N-terminal region located opposite its substrate binding site, although this interaction was not affected by CsA (36). The same region of CypB was later found to be responsible for interaction with ERp72 and Grp94 (32). Interestingly, CypC shares 67% sequence identity and high structural similarity with CypB including a positively charged region near its N terminus (PDB codes 2ESL for CypC and 1CYN for CypB). This suggests that their ER interactomes may be similar, potentially affecting their subcellular localization and their cooperation with functional partners.

We anticipated that combined depletion of CypB and CypC might have a negative impact on folding efficiency and export through the secretory pathway of *cis*-Pro-containing proteins such as albumin and transferrin. This was based on previous experiments in cells in which treatment with CsA or depletion of CypB alone impaired folding, impeded export, or reduced the expression of several secretory or membrane proteins (30, 31, 48). Such phenotypes could arise through several mechanisms including reduced *cis-trans* isomerase activity, a loss of cyclophilin-associated chaperone functions (58) or an alteration in ER interactome dynamics with a consequent impairment in the functions of associated chaperones or folding catalysts. Indeed, we observed a reduced rate of transferrin secretion upon combined CypB and CypC knockdown, consistent with a previous report employing CsA (48). Given this context, we were surprised to observe under the same knockdown conditions an accelerated rate of oxidative folding and secretion for albumin.

Because we showed previously that the oxidative folding of albumin in HepG2 cells was catalyzed in part by PDI and ERp72 (5), we tested the oxidative status of several PDI family members upon CypB and CypC knockdown. For all three PDI members tested, we observed an increase in the proportion of molecules with active sites in the oxidized state, although the majority was still found in reduced forms. Because the oxidized form is required for catalysis of disulfide formation in folding substrates, this shift is a likely contributing factor in the more efficient oxidative folding of albumin.

Why albumin and transferrin are differentially impacted by depletion of cyclophilins B and C is unclear. Potential explanations include inherent differences in the tolerance of each protein for changes in the proline isomerization state or differences in their interactions with the ER quality control machinery, *i.e.* transferrin is glycosylated and binds to ER lectin-chaperones, whereas unglycosylated albumin does not (59). Alternatively, transferrin may have a greater propensity to acquire incorrect disulfides than albumin due to increased PDI member oxidation, which subsequently requires more extensive isomerization prior to secretion. Such incorrect disulfides are not detectable in our assays of oxidative folding (Fig. 3).

How does depletion of ER cyclophilins result in increased oxidation of PDI enzymes? PDI family members contain a *cis*-Pro in proximity to their active sites that is critical for enzymatic activity. We considered that CypB and CypC could potentially regulate the activity of PDIs through isomerization of this residue. However, this possibility is unlikely as suggested by a number of previous studies. For example, cytosolic *Escherichia coli* PPI was shown *in vitro* to improve the oxidative refolding of RNase T1 mediated by bovine liver PDI (60). Similar enhancements in folding rates were observed when PPI was included during oxidative refolding of an Fab antibody fragment mediated by rat ERp72, PDI, or P5 (61) or upon addition of CypB to assays monitoring the ERp72-catalyzed assembly of Ig C_H1-C_L heterodimers (32). However, in all cases, the rate enhancements were found to be substrate specific because they were not observed in refolding experiments using RNase A, another *cis*-Pro-containing substrate. Because the refolding process was shown to depend on the substrate it is likely that PPIs participate directly in substrate refolding by catalyzing the formation of intermediates that are better substrates for PDIs, rather than through a direct regulation of PDI activity. This cooperative action is likely enhanced by the physical association of CypB with several PDI family members (32, 62). In addi-

tion to oxidative refolding studies, CypB was also shown not to regulate the reductase activity of either ERp72 as tested using the fluorescent substrate Di-Eosin-GSSG (32) or PDI in an insulin reduction assay (62). Independently, we also tested the reductase activity of ERp57 in an insulin reduction assay in the absence or presence of recombinant CypB or CypC but failed to observe any differences in ERp57 activity (data not shown).

Given that *in vitro* experiments did not reveal any direct regulatory activity of CypB or CypC on PDI family members, we speculated that the more oxidized state of these enzymes upon CypB and CypC depletion might reflect a more oxidized ER environment. Indeed, the cellular GSSG:GS ratio increased dramatically upon combined depletion of ER cyclophilins. Likewise, CsA treatment, which depletes cyclophilins from the ER via secretion, induced a similar degree of ER hyperoxidation. Oxidative stress associated with CsA treatment has been noted previously and includes an increase in reactive oxygen species, increased membrane lipid peroxidation, and elevated levels of oxidized glutathione (54, 63). We can now demonstrate that a substantial component of this oxidative stress is caused by depletion of CypB and CypC within the ER rather than through CsA inhibition of other cellular cyclophilins or through impaired cytosolic calcineurin signaling. Because the hyperoxidation phenotype associated with CypB and CypC depletion could be recapitulated with CsA treatment, we used the latter to investigate the involvement of candidate oxidant enzymes in the process of ER hyperoxidation. We reasoned that ER cyclophilins might alter the proline isomerization state of these enzymes and either modulate oxidant activity directly or affect the recruitment of potential regulatory factors that bind to alternative *cis*- or *trans*-Pro conformers. We focused on Ero1, PRDX4, VKOR, and QSOX1 and observed that in each case their depletion had no significant impact on CsA-induced hyperoxidation. This was surprising because Ero1, PRDX4, and VKOR have well established roles in ER oxidation (13, 14, 16, 18). The result for QSOX1 is less surprising because previous studies depleting QSOX1 in HepG2 cells could detect no role for the enzyme in the oxidative folding or secretion of albumin nor did it contribute to the recovery of the ER redox balance following a reductive challenge (16). In contrast, recent studies from the Fass group (57) have shown that QSOX1 is primarily secreted from cells and its oxidative activity is required extracellularly for the incorporation of laminin into the extracellular matrix of fibroblasts. This raised the idea that combined CypB and CypC depletion or CsA treatment might impede the secretion of QSOX1, leading to its accumulation in the ER where it causes hyperoxidation. However, we could not detect any reproducible changes in QSOX1 secretion under these conditions (data not shown). Consequently, our findings point to the existence of one or more additional pathways of ER oxidation that are modulated by ER cyclophilins. Candidates include the ER glutathione peroxidases GPx7 and GPx8 that have been shown *in vitro* to catalyze the peroxide-dependent oxidation of the active sites of PDI for subsequent disulfide formation in a reduced and denatured protein substrate (64). Another possibility is dehydroascorbate that can be generated through the oxidation of ascorbate by several ER enzymes and has been shown *in vitro* to oxidize not only the active sites of PDI but also thiols in denatured proteins (65, 66).

CsA has successfully been used as an immunosuppressive drug in solid organ transplantation. However, the dosage of the drug has to be carefully monitored due to adverse toxic side effects, such as nephrotoxicity and hypertension, the underlying mechanism of which is not fully understood but is associated with oxidative stress (54, 63). We have shown that a component of the CsA-induced oxidative stress is due to the attendant depletion of ER-localized CypB and CypC. Consequently, our results contribute to a molecular understanding of the basis for CsA-induced oxidative stress. Future identification of the oxidative pathway affected by cyclophilin depletion may suggest an alternative target for drugs that could help mitigate CsA-induced stress in addition to the use of antioxidants that have proven beneficial in reducing adverse side effects and improving recovery following CsA treatment (63, 67–71).

Acknowledgments—We thank Drs. David Ron, Kathleen Berkner, and Neil Bulleid for their generous gifts of antibodies.

REFERENCES

1. Bagola, K., Mehnert, M., Jarosch, E., and Sommer, T. (2011) Protein dislocation from the ER. *Biochim. Biophys. Acta* **1808,** 925–936
2. Hatahet, F., and Ruddock, L. W. (2009) Protein disulfide isomerase: a critical evaluation of its function in disulfide bond formation. *Antioxid. Redox Signal.* **11,** 2807–2850
3. Jessop, C. E., Chakravarthi, S., Garbi, N., Hämmerling, G. J., Lovell, S., and Bulleid, N. J. (2007) ERp57 is essential for efficient folding of glycoproteins sharing common structural domains. *EMBO J.* **26,** 28–40
4. Kang, K., Park, B., Oh, C., Cho, K., and Ahn, K. (2009) A role for protein disulfide isomerase in the early folding and assembly of MHC class I molecules. *Antioxid. Redox Signal.* **11,** 2553–2561
5. Rutkevich, L. A., Cohen-Doyle, M. F., Brockmeier, U., and Williams, D. B. (2010) Functional relationship between protein disulfide isomerase family members during the oxidative folding of human secretory proteins. *Mol. Biol. Cell* **21,** 3093–3105
6. Soldà, T., Garbi, N., Hämmerling, G. J., and Molinari, M. (2006) Consequences of ERp57 deletion on oxidative folding of obligate and facultative clients of the calnexin cycle. *J. Biol. Chem.* **281,** 6219–6226
7. Oka, O. B., Pringle, M. A., Schopp, I. M., Braakman, I., and Bulleid, N. J. (2013) ERdj5 is the ER reductase that catalyzes the removal of non-native disulfides and correct folding of the LDL receptor. *Mol. Cell* **50,** 793–804
8. Ushioda, R., Hoseki, J., Araki, K., Jansen, G., Thomas, D. Y., and Nagata, K. (2008) ERdj5 is required as a disulfide reductase for degradation of misfolded proteins in the ER. *Science* **321,** 569–572
9. Jessop, C. E., Tavender, T. J., Watkins, R. H., Chambers, J. E., and Bulleid, N. J. (2009) Substrate specificity of the oxidoreductase ERp57 is determined primarily by its interaction with calnexin and calreticulin. *J. Biol. Chem.* **284,** 2194–2202
10. Jessop, C. E., Watkins, R. H., Simmons, J. J., Tasab, M., and Bulleid, N. J. (2009) Protein disulphide isomerase family members show distinct substrate specificity: P5 is targeted to BiP client proteins. *J. Cell Sci.* **122,** 4287–4295
11. Frand, A. R., and Kaiser, C. A. (1998) The ERO1 gene of yeast is required for oxidation of protein dithiols in the endoplasmic reticulum. *Mol. Cell* **1,** 161–170
12. Pollard, M. G., Travers, K. J., and Weissman, J. S. (1998) Ero1p: a novel and ubiquitous protein with an essential role in oxidative protein folding in the endoplasmic reticulum. *Mol. Cell* **1,** 171–182
13. Zito, E., Melo, E. P., Yang, Y., Wahlander, Å., Neubert, T. A., and Ron, D. (2010) Oxidative protein folding by an endoplasmic reticulum-localized peroxiredoxin. *Mol. Cell* **40,** 787–797

14. Bulleid, N. J., and Ellgaard, L. (2011) Multiple ways to make disulfides. *Trends Biochem. Sci.* **36,** 485–492
15. Cao, Z., Tavender, T. J., Roszak, A. W., Cogdell, R. J., and Bulleid, N. J. (2011) Crystal structure of reduced and of oxidized peroxiredoxin IV enzyme reveals a stable oxidized decamer and a non-disulfide-bonded intermediate in the catalytic cycle. *J. Biol. Chem.* **286,** 42257–42266
16. Rutkevich, L. A., and Williams, D. B. (2012) Vitamin K epoxide reductase contributes to protein disulfide formation and redox homeostasis within the endoplasmic reticulum. *Mol. Biol. Cell* **23,** 2017–2027
17. Li, W., Schulman, S., Dutton, R. J., Boyd, D., Beckwith, J., and Rapoport, T. A. (2010) Structure of a bacterial homologue of vitamin K epoxide reductase. *Nature* **463,** 507–512
18. Schulman, S., Wang, B., Li, W., and Rapoport, T. A. (2010) Vitamin K epoxide reductase prefers ER membrane-anchored thioredoxin-like redox partners. *Proc. Natl. Acad. Sci. U.S.A.* **107,** 15027–15032
19. Jin, D. Y., Tie, J. K., and Stafford, D. W. (2007) The conversion of vitamin K epoxide to vitamin K quinone and vitamin K quinone to vitamin K hydroquinone uses the same active site cysteines. *Biochemistry* **46,** 7279–7283
20. Kodali, V. K., and Thorpe, C. (2010) Oxidative protein folding and the Quiescin-sulfhydryl oxidase family of flavoproteins. *Antioxid. Redox Signal.* **13,** 1217–1230
21. Flanagan, W. M., Corthésy, B., Bram, R. J., and Crabtree, G. R. (1991) Nuclear association of a T-cell transcription factor blocked by FK-506 and cyclosporin A. *Nature* **352,** 803–807
22. Liu, J., Farmer, J. D., Jr., Lane, W. S., Friedman, J., Weissman, I., and Schreiber, S. L. (1991) Calcineurin is a common target of cyclophilin-cyclosporin A and FKBP-FK506 complexes. *Cell* **66,** 807–815
23. Lang, K., Schmid, F. X., and Fischer, G. (1987) Catalysis of protein folding by prolyl isomerase. *Nature* **329,** 268–270
24. Lu, K. P., Finn, G., Lee, T. H., and Nicholson, L. K. (2007) Prolyl cis-trans isomerization as a molecular timer. *Nat. Chem. Biol.* **3,** 619–629
25. Fischer, G., and Aumüller, T. (2003) Regulation of peptide bond cis/trans isomerization by enzyme catalysis and its implication in physiological processes. *Rev. Physiol. Biochem. Pharmacol.* **148,** 105–150
26. Price, E. R., Zydowsky, L. D., Jin, M. J., Baker, C. H., McKeon, F. D., and Walsh, C. T. (1991) Human cyclophilin B: a second cyclophilin gene encodes a peptidyl-prolyl isomerase with a signal sequence. *Proc. Natl. Acad. Sci. U.S.A.* **88,** 1903–1907
27. Price, E. R., Jin, M., Lim, D., Pati, S., Walsh, C. T., and McKeon, F. D. (1994) Cyclophilin B trafficking through the secretory pathway is altered by binding of cyclosporin A. *Proc. Natl. Acad. Sci. U.S.A.* **91,** 3931–3935
28. Davis, E. C., Broekelmann, T. J., Ozawa, Y., and Mecham, R. P. (1998) Identification of tropoelastin as a ligand for the 65-kDa FK506-binding protein, FKBP65, in the secretory pathway. *J. Cell Biol.* **140,** 295–303
29. Ishikawa, Y., Vranka, J., Wirz, J., Nagata, K., and Bächinger, H. P. (2008) The rough endoplasmic reticulum-resident FK506-binding protein FKBP65 is a molecular chaperone that interacts with collagens. *J. Biol. Chem.* **283,** 31584–31590
30. Colley, N. J., Baker, E. K., Stamnes, M. A., and Zuker, C. S. (1991) The cyclophilin homolog ninaA is required in the secretory pathway. *Cell* **67,** 255–263
31. Bergeron, M. J., Bürzle, M., Kovacs, G., Simonin, A., and Hediger, M. A. (2011) Synthesis, maturation, and trafficking of human Na^+-dicarboxylate cotransporter NaDC1 requires the chaperone activity of cyclophilin B. *J. Biol. Chem.* **286,** 11242–11253
32. Jansen, G., Määttänen, P., Denisov, A. Y., Scarffe, L., Schade, B., Balghi, H., Dejgaard, K., Chen, L. Y., Muller, W. J., Gehring, K., and Thomas, D. Y. (2012) An interaction map of endoplasmic reticulum chaperones and foldases. *Mol. Cell Proteomics* **11,** 710–723
33. Feige, M. J., Groscurth, S., Marcinowski, M., Shimizu, Y., Kessler, H., Hendershot, L. M., and Buchner, J. (2009) An unfolded CH1 domain controls the assembly and secretion of IgG antibodies. *Mol. Cell* **34,** 569–579
34. Bernasconi, R., Soldà, T., Galli, C., Pertel, T., Luban, J., and Molinari, M. (2010) Cyclosporine A-sensitive, cyclophilin B-dependent endoplasmic reticulum-associated degradation. *PLoS One* **5,** e13008
35. Meunier, L., Usherwood, Y. K., Chung, K. T., and Hendershot, L. M. (2002) A subset of chaperones and folding enzymes form multiprotein complexes in endoplasmic reticulum to bind nascent proteins. *Mol. Biol. Cell* **13,** 4456–4469
36. Kozlov, G., Bastos-Aristizabal, S., Määttänen, P., Rosenauer, A., Zheng, F., Killikelly, A., Trempe, J. F., Thomas, D. Y., and Gehring, K. (2010) Structural basis of cyclophilin B binding by the calnexin/calreticulin P-domain. *J. Biol. Chem.* **285,** 35551–35557
37. Stam, N. J., Spits, H., and Ploegh, H. L. (1986) Monoclonal antibodies raised against denatured HLA-B locus heavy chains permit biochemical characterization of certain HLA-C locus products. *J. Immunol.* **137,** 2299–2306
38. Zhang, Y., Baig, E., and Williams, D. B. (2006) Functions of ERp57 in the folding and assembly of major histocompatibility complex class I molecules. *J. Biol. Chem.* **281,** 14622–14631
39. Zito, E., Chin, K. T., Blais, J., Harding, H. P., and Ron, D. (2010) ERO1-β, a pancreas-specific disulfide oxidase, promotes insulin biogenesis and glucose homeostasis. *J. Cell Biol.* **188,** 821–832
40. Rishavy, M. A., Usubalieva, A., Hallgren, K. W., and Berkner, K. L. (2011) Novel insight into the mechanism of the vitamin K oxidoreductase (VKOR): electron relay through Cys43 and Cys51 reduces VKOR to allow vitamin K reduction and facilitation of vitamin K-dependent protein carboxylation. *J. Biol. Chem.* **286,** 7267–7278
41. Rudolf, J., Pringle, M. A., and Bulleid, N. J. (2013) Proteolytic processing of QSOX1A ensures efficient secretion of a potent disulfide catalyst. *Biochem. J.* **454,** 181–190
42. Petersen, T. N., Brunak, S., von Heijne, G., and Nielsen, H. (2011) SignalP 4.0: discriminating signal peptides from transmembrane regions. *Nat. Methods* **8,** 785–786
43. Bram, R. J., Hung, D. T., Martin, P. K., Schreiber, S. L., and Crabtree, G. R. (1993) Identification of the immunophilins capable of mediating inhibition of signal transduction by cyclosporin A and FK506: roles of calcineurin binding and cellular location. *Mol. Cell. Biol.* **13,** 4760–4769
44. Friedman, J., and Weissman, I. (1991) Two cytoplasmic candidates for immunophilin action are revealed by affinity for a new cyclophilin: one in the presence and one in the absence of CsA. *Cell* **66,** 799–806
45. Arber, S., Krause, K. H., and Caroni, P. (1992) s-cyclophilin is retained intracellularly via a unique COOH-terminal sequence and colocalizes with the calcium storage protein calreticulin. *J. Cell Biol.* **116,** 113–125
46. Fearon, P., Lonsdale-Eccles, A. A., Ross, O. K., Todd, C., Sinha, A., Allain, F., and Reynolds, N. J. (2011) Keratinocyte secretion of cyclophilin B via the constitutive pathway is regulated through its cyclosporin-binding site. *J. Invest. Dermatol.* **131,** 1085–1094
47. Bull, V. H., and Thiede, B. (2012) Proteome analysis of tunicamycin-induced ER stress. *Electrophoresis* **33,** 1814–1823
48. Lodish, H. F., and Kong, N. (1991) Cyclosporin A inhibits an initial step in folding of transferrin within the endoplasmic reticulum. *J. Biol. Chem.* **266,** 14835–14838
49. Mezghrani, A., Fassio, A., Benham, A., Simmen, T., Braakman, I., and Sitia, R. (2001) Manipulation of oxidative protein folding and PDI redox state in mammalian cells. *EMBO J.* **20,** 6288–6296
50. Appenzeller-Herzog, C., Riemer, J., Zito, E., Chin, K. T., Ron, D., Spiess, M., and Ellgaard, L. (2010) Disulphide production by Ero1α-PDI relay is rapid and effectively regulated. *EMBO J.* **29,** 3318–3329
51. Appenzeller-Herzog, C., Riemer, J., Christensen, B., Sørensen, E. S., and Ellgaard, L. (2008) A novel disulphide switch mechanism in Ero1α balances ER oxidation in human cells. *EMBO J.* **27,** 2977–2987
52. Go, Y. M., and Jones, D. P. (2008) Redox compartmentalization in eukaryotic cells. *Biochim. Biophys. Acta* **1780,** 1273–1290
53. Krauskopf, A., Buetler, T. M., Nguyen, N. S., Macé, K., and Ruegg, U. T. (2002) Cyclosporin A-induced free radical generation is not mediated by cytochrome P-450. *Br. J. Pharmacol.* **135,** 977–986
54. Lee, J. (2010) Use of antioxidants to prevent cyclosporine a toxicity. *Toxicol. Res.* **26,** 163–170
55. Pérez de Hornedo, J., de Arriba, G., Calvino, M., Benito, S., and Parra, T. (2007) Cyclosporin A causes oxidative stress and mitochondrial dysfunction in renal tubular cells. *Nefrologia* **27,** 565–573
56. Watkins, P. B. (1990) The role of cytochromes P-450 in cyclosporine metabolism. *J. Am. Acad. Dermatol.* **23,** 1301–1309; discussion 1309–1311
57. Ilani, T., Alon, A., Grossman, I., Horowitz, B., Kartvelishvily, E., Cohen,

S. R., and Fass, D. (2013) A secreted disulfide catalyst controls extracellular matrix composition and function. *Science* **341,** 74–76
58. Barik, S. (2006) Immunophilins: for the love of proteins. *Cell Mol. Life Sci.* **63,** 2889–2900
59. Ou, W. J., Cameron, P. H., Thomas, D. Y., and Bergeron, J. J. (1993) Association of folding intermediates of glycoproteins with calnexin during protein maturation. *Nature* **364,** 771–776
60. Schönbrunner, E. R., and Schmid, F. X. (1992) Peptidyl-prolyl cis-trans isomerase improves the efficiency of protein disulfide isomerase as a catalyst of protein folding. *Proc. Natl. Acad. Sci. U.S.A.* **89,** 4510–4513
61. Rupp, K., Birnbach, U., Lundström, J., Van, P. N., and Söling, H. D. (1994) Effects of CaBP2, the rat analog of ERp72, and of CaBP1 on the refolding of denatured reduced proteins: comparison with protein disulfide isomerase. *J. Biol. Chem.* **269,** 2501–2507
62. Horibe, T., Yosho, C., Okada, S., Tsukamoto, M., Nagai, H., Hagiwara, Y., Tujimoto, Y., and Kikuchi, M. (2002) The chaperone activity of protein disulfide isomerase is affected by cyclophilin B and cyclosporin A *in vitro*. *J. Biochem.* **132,** 401–407
63. Wolf, A., Trendelenburg, C. F., Diez-Fernandez, C., Prieto, P., Houy, S., Trommer, W. E., and Cordier, A. (1997) Cyclosporine A-induced oxidative stress in rat hepatocytes. *J. Pharmacol. Exp. Ther.* **280,** 1328–1334
64. Nguyen, V. D., Saaranen, M. J., Karala, A. R., Lappi, A. K., Wang, L., Raykhel, I. B., Alanen, H. I., Salo, K. E., Wang, C. C., and Ruddock, L. W. (2011) Two endoplasmic reticulum PDI peroxidases increase the efficiency of the use of peroxide during disulfide bond formation. *J. Mol. Biol.* **406,** 503–515
65. Margittai, E., and Bánhegyi, G. (2010) Oxidative folding in the endoplasmic reticulum: towards a multiple oxidant hypothesis? *FEBS Lett.* **584,** 2995–2998
66. Ruddock, L. W. (2012) Low-molecular-weight oxidants involved in disulfide bond formation. *Antioxid. Redox Signal.* **16,** 1129–1138
67. Zhong, Z., Arteel, G. E., Connor, H. D., Yin, M., Frankenberg, M. V., Stachlewitz, R. F., Raleigh, J. A., Mason, R. P., and Thurman, R. G. (1998) Cyclosporin A increases hypoxia and free radical production in rat kidneys: prevention by dietary glycine. *Am. J. Physiol.* **275,** F595–604
68. Tariq, M., Morais, C., Sobki, S., Al Sulaiman, M., and Al Khader, A. (1999) *N*-Acetylcysteine attenuates cyclosporin-induced nephrotoxicity in rats. *Nephrol. Dial. Transplant.* **14,** 923–929
69. Wang, C., and Salahudeen, A. K. (1994) Cyclosporine nephrotoxicity: attenuation by an antioxidant-inhibitor of lipid peroxidation *in vitro* and *in vivo*. *Transplantation* **58,** 940–946
70. de Lorgeril, M., Boissonnat, P., Salen, P., Monjaud, I., Monnez, C., Guidollet, J., Ferrera, R., Dureau, G., Ninet, J., and Renaud, S. (1994) The beneficial effect of dietary antioxidant supplementation on platelet aggregation and cyclosporine treatment in heart transplant recipients. *Transplantation* **58,** 193–195
71. Louhelainen, M., Merasto, S., Finckenberg, P., Lapatto, R., Cheng, Z. J., and Mervaala, E. M. (2006) Lipoic acid supplementation prevents cyclosporine-induced hypertension and nephrotoxicity in spontaneously hypertensive rats. *J. Hypertens.* **24,** 947–956